

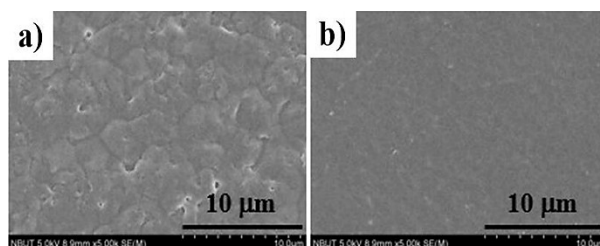
Synergistic effects of filler-migration and moisture on the surface structure of polyamide 6 composites under electric field

Qi Zhou,<sup>1, \*</sup> Jingjing Zhang,<sup>1,2</sup> Yuanyu Wang,<sup>1</sup> Weidong Wang,<sup>1</sup> Shunying Yao,<sup>1</sup>  
Yang Cong,<sup>1</sup> Jianghua Fang<sup>1</sup>

<sup>1</sup>School of Materials and Chemical Engineering, Ningbo University of Technology,  
Ningbo 315016, People Republic of China

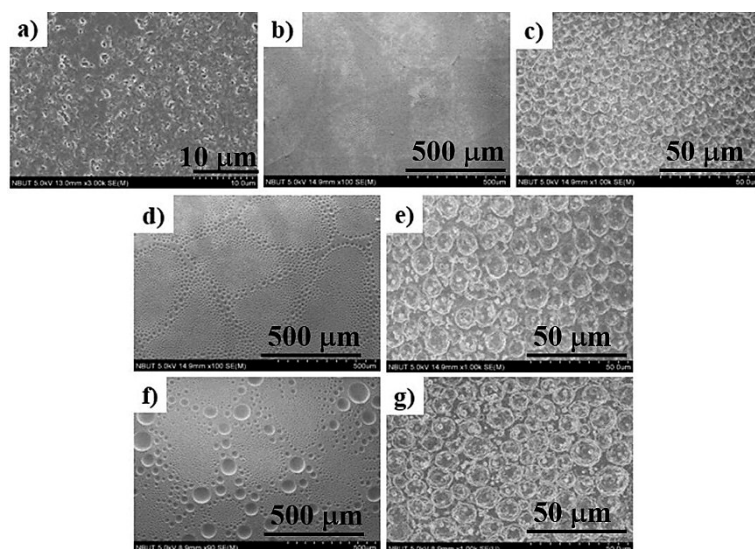
<sup>2</sup>Department of Polymer Science and Engineering, School of Material Science and  
Chemical Engineering, Ningbo University, Ningbo, 315211, Zhejiang. P. R. China.

\*Corresponding author: Qi Zhou, E-mail address: [zhouqi@nbut.cn](mailto:zhouqi@nbut.cn)



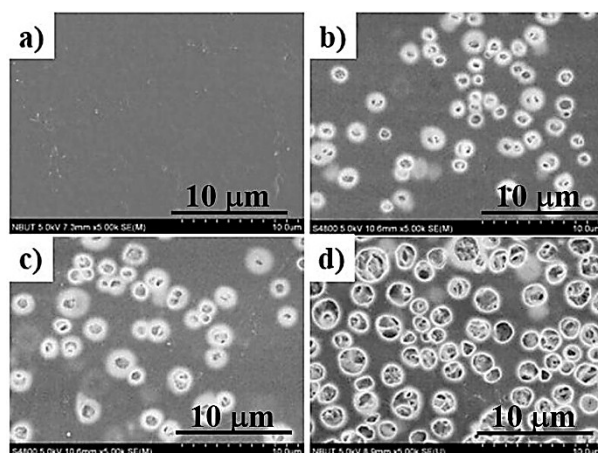
**Figure S1** The structure and morphology of PA6 synthesized at 20% of humidity. a) The morphology of air side; b) The morphology of bottom side

Figure S1 shows the structure and morphology of PA6 synthesized at 20% of humidity. It has similar results with that of sample synthesized at 40% of moisture. Thus, the moisture below 40% is not further discussed.



**Figure S2** SEM images of air-side of PA6/PGN samples prepared at different moisture and magnification: a) 40%, 3K; b) 55%, 90; c) 55%, 1K; d) 70%, 90; e) 70%, 1K; f) 85%, 90 and g) 85%, 1K.

Figure S2 shows the SEM images of air-side of PA6/PGN samples. At the low humidity, the surface has some micro-voids on top. However, when the humidity reaches 55%, the surface shows disorder and porous structure as shown in Figure S2 b,c. Further increase of the moisture, concaves are formed along the edge of the cellular pore, and the inner pore size does not change much. The bottom-side morphology of the PA6/PGN composites is shown in Figure S3. The morphology of the bottom side is relatively flat due to the substrate effect. The samples prepared at the low moisture are quite smooth without any micro-voids or pores. However, more pores appear when the humidity rises to 55%.



**Figure S3** SEM images of bottom-side of PA6/PGN samples prepared at different moisture and magnification: a) 40%, 5K; b) 55%, 5K; c) 70%, 5K and d) 85%, 5K.

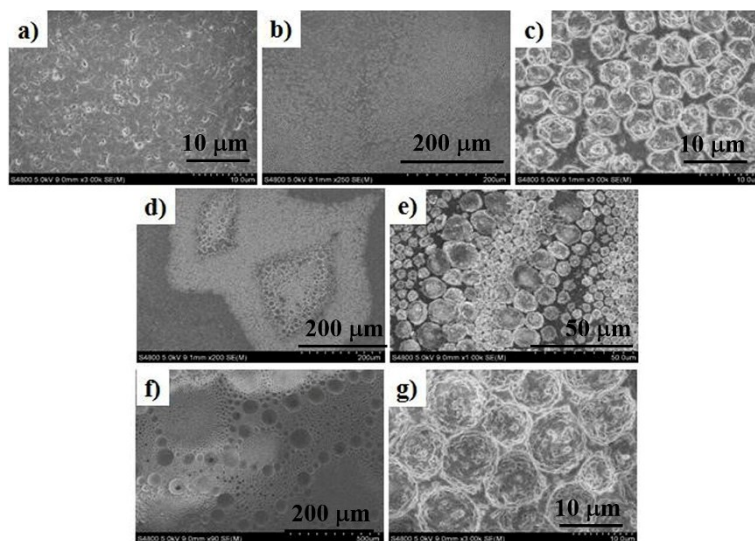


**Figure S4** SEM images of air-side of PA6/ABPOSS samples prepared at different moisture and magnification: a) 40%, 3K; b) 55%, 250; c) 55%, 3K; d) 70%, 90; e) 70%, 200; f) 85%, 90 and g) 85%, 3K.

Figure S4 shows the SEM images of air-side of PA6/AB-POSS samples. It is found that the air-side morphology of PA6/AB-POSS composites is much rougher than that of pure PA6 and PA6/PGN synthesized at the high moisture. The aggregation of AB-POSS may hinder the distribution of water molecules on the air-solid interface which can make the pores more heterogeneous. The more porous structure can be observed at the bottom side, especially in the high moisture case (Figure S5). This may indicate that the AB-POSS cannot stabilize the water droplet which can make it sediment to the bottom side.

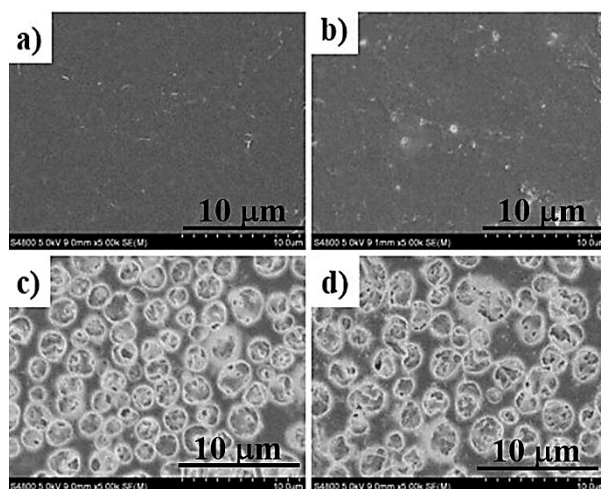


**Figure S5** SEM images of bottom-side of PA6/ABPOSS samples prepared at different moisture and magnification: a) 40%, 3K; b) 55%, 3K; c) 70%, 3K and d) 85%, 3K.

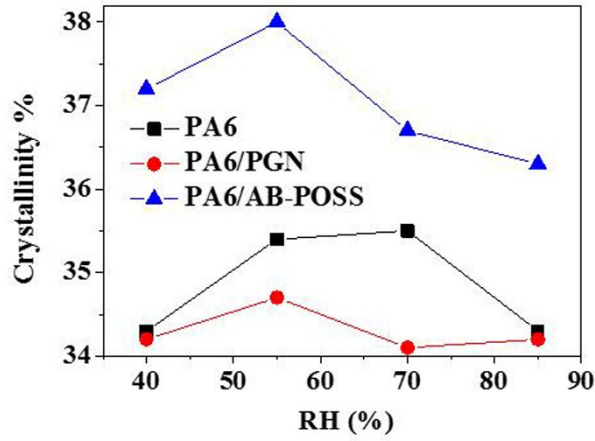


**Figure S6** The crystallinity of PA6 and its composites.

The heat enthalpy of PA6 and its composites were measured by a differential scanning calorimeter (DSC Q2000, TA Instruments) in a nitrogen atmosphere. The samples were heated from 0°C to 250°C at 10°C /min. The heat of fusion, which was determined by integrating the heat flow from 200 to 230°C, was used to calculate the level of crystallinity based on the following formula:

$$X_c(\%) = \frac{\Delta H_m}{(1 - \Phi)\Delta H_m^0} \times 100 \quad (1)$$

where  $\Delta H_m$  is the heat enthalpy of the sample,  $\Delta H_m^0$  is the enthalpy corresponding to the melting of 100% crystalline PA6, which is taken as 230 J/g, and  $\Phi$  is the weight fraction of AB-POSS or PGN in the composites.